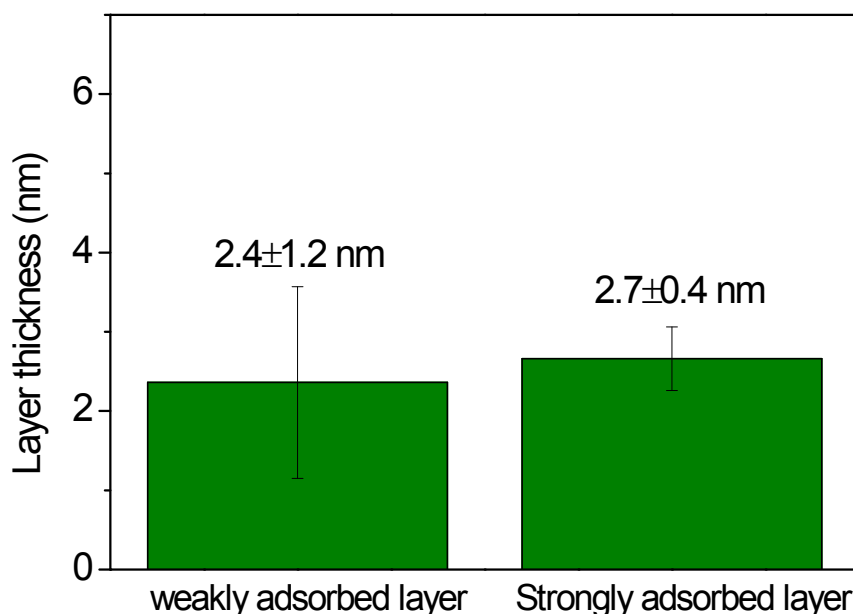


## Supporting Information

### Observing Different Dynamic Behaviors of Weakly and Strongly Adsorbed Polystyrene Chains at Interfaces

Xu Li<sup>1</sup>, Xiaofeng Han<sup>1</sup>, Xiaoliang Wang<sup>2</sup>, Zhan Chen<sup>3\*</sup>, and Xiaolin Lu<sup>1\*</sup>

We applied a film thickness gauge (SCREEN SPE USA, LLC, Lambda Ace VM-1200) to measure the PS layer thicknesses. For the weakly adsorbed layer, the measured thickness was  $2.4 \pm 1.2$  nm; and for the strongly adsorbed layer, the measured thickness was  $2.7 \pm 0.4$  nm, as shown in Figure S1. The results are consistent with the reported data in the literatures.<sup>S1,S2</sup>



**Figure S1.** The thicknesses of weakly and strongly adsorbed layers measured by a film thickness gauge (each averaged from three independent measurements).

In Figure S2, the interfacial deuterated water ( $D_2O$ ) spectra were shown for both the weakly and strongly adsorbed layers in *ssp* polarization combination. The results

indicated that D<sub>2</sub>O were orderly arranged at the interface for both layers.

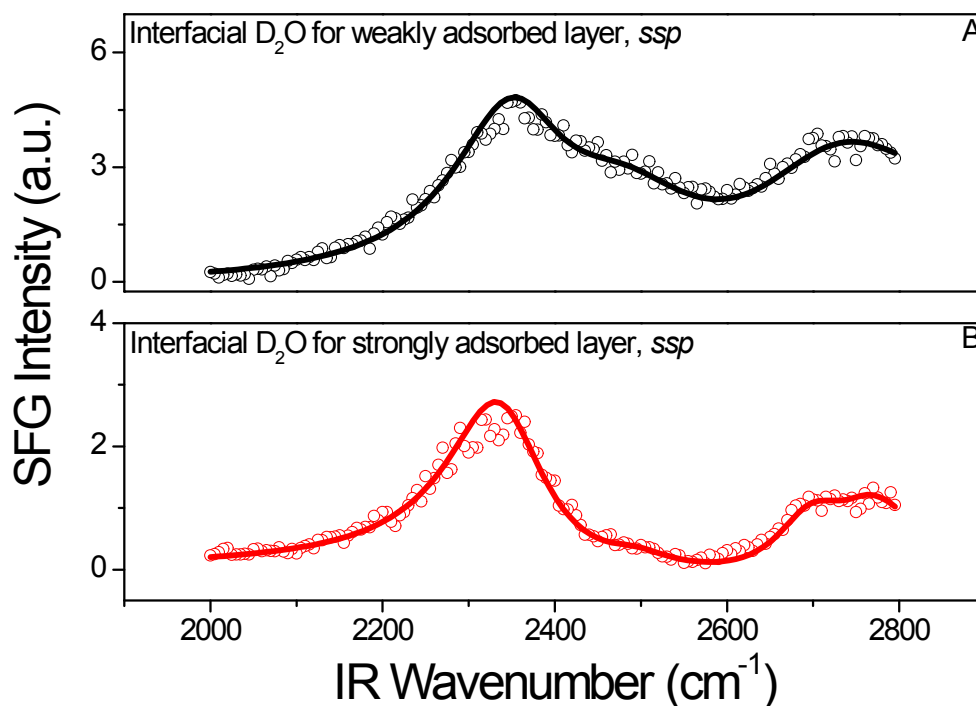


**Figure S2.** Normalized SFG spectra of the weakly and strongly adsorbed layers on sapphire in contact with D<sub>2</sub>O in the OD stretching frequency range with *ssp* polarization combination. Panel A shows the spectrum of D<sub>2</sub>O for the weakly adsorbed layer and Panel B shows the spectrum of D<sub>2</sub>O for the strongly adsorbed layer. The solid lines were plotted to guide eyes.

We also collected SFG spectrum from the pure sapphire/air interface, as shown in Figure S3. A sharp peak located at ~3720 cm<sup>-1</sup> was observed, which can be assigned to the free OH vibrational mode on the sapphire surface.<sup>S3-S5</sup>

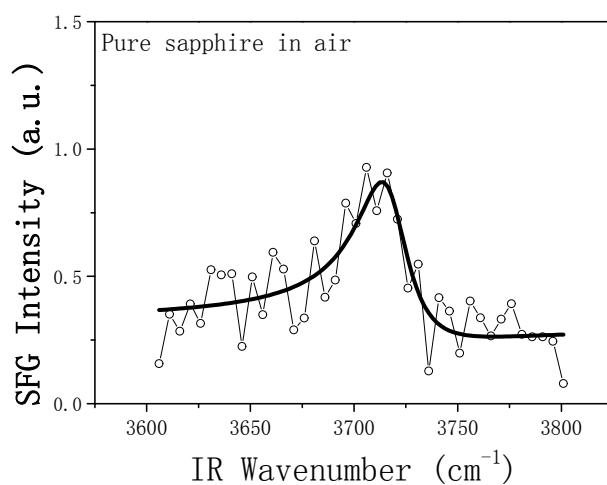


**Figure S3.** Normalized SFG spectrum of pure sapphire in air in OH stretching

frequency range.

Lorentz equation was used for fitting SFG spectra. When the IR frequency is near the vibrational resonance,  $\chi_{eff}^{(2)}$  can be written as<sup>S6,S7</sup>:

$$\chi_{eff}^{(2)} = \chi_{nr} + \sum_q \frac{A_q}{w_2 - w_q + i\Gamma_q} \quad (S1)$$

where  $\chi_{nr}$  represents the nonresonant background contribution.  $A_q$ ,  $w_q$  and  $\Gamma_q$  represent the amplitude, resonant frequency and damping coefficient of the  $q$ th vibrational mode, respectively. In Table S1, fitting results were listed for the SFG spectra presented in the main context. In Table S2, the refractive indices of sum-frequency, Vis, and IR beams were listed. In Table S3, the calculated interfacial Fresnel coefficients were listed.

**Table S1.** The fitting results of the SFG spectra presented in the main text.

$\omega_q$ (cm <sup>-1</sup> )	$\Gamma_q$ (cm <sup>-1</sup> )	Assignment	on sapphire (air)		on sapphire (D <sub>2</sub> O)		on sapphire (CCl <sub>4</sub> )	
			weakly	strongly	weakly	strongly	weakly	strongly
			$A_{ssp}$	$A_{ssp}$	$A_{ssp}$	$A_{ssp}$	$A_{ssp}$	$A_{ssp}$
2850	10.5	CH <sub>2</sub> ss	3.2	6.0	-	5.5	2.8	8.5
2875	12.3	CH <sub>3</sub> ss	7.1	5.4	-	3.7	8.5	5.8
2910	10.0	CH	4.0	6.3	-	3.2	2.5	6.0
2935	11.5	CH <sub>2</sub> as	-7.2	-7.6	-	-6.5	-13.4	-10.8
2945	8.0	CH <sub>3</sub> Fermi	1.5	-	-	-	-	-
3023	9.0	$\nu_{20b}$						
3032	7.0	$\nu_{7a}$	-	-5.8	-	-	-	-
3050	6.0	$\nu_{7b}$	-	4.4	-	-	-	-
3065	6.0	$\nu_2$	-	8.8	-	-	-	-
3620	80.0	OH	-	-	-	84.1	-	-
3660	80.0	OH	53.2	110.0	-	-	70.7	431.0

**Table S2.** Refractive indexes of Sum-frequency, Vis, and IR beams

Medium	Refractive indexes at sum frequency	Refractive indexes at visible frequency	Refractive indexes at infrared frequency (2955 cm <sup>-1</sup> )
Air	1.00	1.00	1.00
D <sub>2</sub> O	1.33	1.33	1.32
Sapphire	1.78	1.77	1.70
PS adsorbed layer	1.20	1.20	1.20
CCl <sub>4</sub>	1.46	1.46	1.44

Note: the refractive indexes were referred to references S8, S9 and S10.

**Table S3.** The calculated Fresnel coefficient values

	$F_{ssp-yyz}/ F_{ssp-yyz} $
Sapphire (PS)/Air	-0.21+0.05i/0.22
Sapphire (PS)/D <sub>2</sub> O	-0.38-0.36i/0.52
Sapphire (PS)/CCl <sub>4</sub>	0.02-0.57i/0.57

## REFERENCES

- S1. Gin, P.; Jiang, N.; Liang, C.; Taniguchi, T.; Akgun, B.; Satija, S. K.; Endoh, M. K.; Koga, T. Revealed Architectures of Adsorbed Polymer Chains at Solid-Polymer Melt Interfaces. *Phys. Rev. Lett.* 2012, *109*, 265501.
- S2. Sen, M.; Jiang, N.; Cheung, J.; Endoh, M. K.; Koga, T.; Kawaguchi, D.; Tanaka, K. Flattening Process of Polymer Chains Irreversibly Adsorbed on a Solid. *ACS Macro Lett.* **2016**, *5*, 204–508.
- S3. Nanjundiah, K.; Hsu, P. Y.; Dhinojwala, A. Understanding Rubber Friction in the Presence of Water Using Sum-Frequency Generation Spectroscopy. *J. Chem. Phys.* **2009**, *130*, 024702.
- S4. Hass, K. C.; Schneider, W. F.; Curioni, A.; Andreoni, W. The Chemistry of Water on Alumina Surfaces: Reaction Dynamics from First Principles. *Science* **1998**, *282*, 265–268.
- S5. Kurian, A.; Prasad, S.; Dhinojwala, A. Direct Measurement of Acid–Base Interaction Energy at Solid Interfaces. *Langmuir* **2010**, *26*, 17804–17807.

- S6. Wang, J.; Chen, C.; Buck, S. M.; Chen, Z. Molecular Chemical Structure on Poly (methyl methacrylate)(PMMA) Surface Studied by Sum Frequency Generation (SFG) Vibrational Spectroscopy. *J. Phys. Chem. B* **2001**, *105*, 12118–12125.
- S7. Li, X.; Li, B.; Zhang, X.; Li, C.; Guo, Z.; Zhou, D.; Lu, X. Detecting Surface Hydration of Poly(2-hydroxyethyl methacrylate) in Solution *in situ*. *Macromolecules* **2016**, *49*, 3116–3125.
- S8. See the website “<https://refractiveindex.info>”.
- S9. Zhuang, X.; Miranda, P. B.; Kim, D.; Shen, Y. R. Mapping molecular orientation and conformation at interfaces by surface nonlinear optics. *Phys. Rev. B* **1999**, *59*, 12632–12640.
- S10. Simpson, G. J.; Dailey, C. A.; Plocinik, R. M.; Moad, A. J.; Polizzi, M. A.; Everly, R. M. Direct Determination of Effective Interfacial Optical Constants by Nonlinear Optical Null Ellipsometry of Chiral Films. *Anal. Chem.* **2005**, *77*, 215–224.